

# Model-based chatter stability prediction and detection for the turning of a flexible workpiece

Kaibo Lu<sup>1\*</sup>, Zisheng Lian<sup>1</sup>, Fengshou Gu<sup>1,2</sup>, Hunju Liu<sup>1</sup>

1. College of Mechanical Engineering, Taiyuan University of Technology, Shanxi 030024, P.R. China

2. School of Computing and Engineering, University of Huddersfield, Huddersfield, HD1 3DH, UK

\* Corresponding author. Email: [lvkaibo@tyut.edu.cn](mailto:lvkaibo@tyut.edu.cn); Tel: +86-139-0341-8795

## Abstract

Machining long slender workpieces still presents a technical challenge on the shop floor due to their low stiffness and damping. Regenerative chatter is a major hindrance in machining processes, reducing the geometric accuracies and dynamic stability of the cutting system. This study has been motivated by the fact that chatter occurrence is generally in relation to the cutting position in straight turning of slender workpieces, which has seldom been investigated comprehensively in literature. In the present paper, a predictive chatter model of turning a tailstock supported slender workpiece considering the cutting position change during machining is explored. Based on linear stability analysis and stiffness distribution at different cutting positions along the workpiece, the effect of the cutting tool movement along the length of the workpiece on chatter stability is studied. As a result, an entire stability chart for a single cutting pass is constructed. Through this stability chart the critical cutting condition and the chatter onset location along the workpiece in a turning operation can be estimated. The difference between the predicted tool locations and the experimental results was within 9% at high speed cutting. Also, on the basis of the predictive model the dynamic behavior during chatter that when chatter arises at some cutting location it will continue for a period of time until another specified location is arrived at, can be inferred. The experimental observation was in good agreement with the theoretical inference. Moreover, it is shown that vibration spectrum is more sensitive to the chatter evolution than the signal variance. Specifically, when the cutting operation transfers from stable to unstable state, the corresponding vibration frequency features a shift from the spindle rotation frequency or its harmonics to the critical chatter frequency that slightly varies during the chatter-lasting period.

**Keywords:** Chatter; Stability; Turning; Flexible workpieces; Chatter detection.

## Nomenclature

|           |  |
|-----------|--|
| $A$       | Cross sectional area of the workpiece (mm <sup>2</sup> )       |
| $d$       | Depth of cut ( <i>doc</i> ) for a single cutting pass (mm)     |
| $d_{lim}$ | Critical <i>doc</i> (mm)                                       |
| $C$       | Damping coefficient  |
| $D$       | Diameter of workpiece (mm)                                     |
| $E$       | Young's modulus (MPa)  |
| $f$       | Feedrate of the tool (mm/rev)                                  |
| $f_c$     | Critical chatter frequency (Hz)                                |
| $f_{SR}$  | Spindle rotation frequency (Hz)                                |
| $F$       | Cutting force (N)  |
| $I$       | Moment of inertia of the work cross section (mm <sup>4</sup> ) |
| $k_e$     | Equivalent stiffness (N/m)                                     |
| $K_f$     | Cutting force coefficient (N/mm <sup>2</sup> )                 |
| $k^*$     | Non-dimensional $z$ -coordinate                                |
| $L$       | Length of workpiece (mm)                                       |

|                        |  |
|------------------------|--|
| $\min(d_{\text{lim}})$ | Minimum critical <i>doc</i> (mm)                       |
| $M_1, M_2, M_3, M_4$   | Configurable parameters for chatter detection          |
| $s^*$                  | Length-to-diameter ratio                               |
| $T$                    | Time delay (s)   |
| $T_j(t)$               | Generalized coordinate in the $j$ th mode              |
| $(v_1)_{cr}$           | First critical feedrate (mm/rev)                       |
| $W_j(z)$               | The $j$ th normal mode                                 |
| $X, Y, Z$              | Coordinate axes  |
| $\alpha_j, B_j, R_j$   | Constants related to the $j$ th normal mode            |
| $\delta(z, t)$         | Impulse function                                       |
| $\zeta$                | Equivalent damping ratio                               |
| $\mu$                  | Overlap factor   |
| $\mu^*$                | Non-dimensional feedrate of the cutting tool           |
| $\rho$                 | Density of the workpiece                               |
| $\tau^*$               | Non-dimensional time                                   |
| $\omega$               | Chatter frequency (rad/s)                              |
| $\omega_d$             | Frequency of damped vibration (rad/s)                  |
| $\omega_n$             | Natural frequency of the vibration system (rad/s)      |
| $\Omega$               | Rotational speed of spindle (rpm)                      |
| Subscript              |  |
| $j$                    | Corresponding to the $j$ th normal mode of a workpiece |

## 1. Introduction

Chatter, the violent dynamic motion occurring between the machine tool and the workpiece in a machining process, is often encountered in turning of a long slender workpiece. It not only reduces the machining accuracy but also causes damages to machine tools. Therefore, many investigations have been carried out to predict and thereby take adequate measures to avoid it during a machining process. Largely, the investigations can be viewed into two main categories: chatter stability analysis [1, 2] and chatter monitoring and control [3, 4].

Chatter vibrations result from the interaction between the metal cutting process and the workpiece or machine tool structure. According to the relative flexibility of the workpiece and the cutting tool, different chatter models were formulated. In the earlier chatter studies, the turning tool was often modeled as a single lumped vibration system for representing the motion of the orthogonal facing or grooving processes [5, 6]. Apparently, it is a time-invariant single degree of freedom (SDOF) chatter model if the tool wear factor [7] is not included. By calculating the corresponding mathematical expressions using analytical or numerical methods, the chatter stability lobes of the cutting system that plot the boundary between the stable and unstable zones with respect to the spindle speed and the width or depth of cut (*doc*), can be obtained. On the contrary, if the flexibility of the workpiece is predominant, the cutting tool can be assumed to be rigid. In this case the flexible workpiece was generally modeled as an SDOF model [8], a continuous system [9], or a finite element model [10, 11] to analyze chatter onset using Nyquist criterion.

In the past years, many researchers took into account the compliance between the cutting tool and the workpiece in chatter stability prediction. Chen and Tsao [12, 13] formulated a 2DOF dynamic chatter model for modeling an orthogonal cutting process with and without the tailstock supported flexible workpieces. The workpiece is regarded as a continuous Euler-Bernoulli beam, in which only the first mode shape is accounted in the compliant chatter model. The simulation results have demonstrated that the critical chip width of the deformed work case is constantly larger than the rigid body case. Vela-Martinez et al. [14] introduced a multiple degrees of freedom chatter model based on the compliance between the tool and the workpiece. The experimental validation was absent in the study. Sekar et al. [15] conducted machining experiments in the case that the tool cut the workpiece at a fixed position to

verify a compliant 2DOF chatter model. The influence of the various cutting positions on the frequency response function and chatter stability was investigated in [16]. Recently, Otto et al. [17] extended the number of the mode shapes of Chen and Tsao's compliant model and analyzed the influence of cutting positions on chatter stability theoretically.

Technically, chatter stability prediction cannot completely eliminate chatter occurrence in practice. Hence, detection of predicted chatter stability with sensors to acquire force, vibration, acoustic emission, power or current signals from a machining process becomes necessary. Cutting forces enable to represent the cutting status directly whereas the installation of force transducers is unfavorable to the original machine tool structures. Vibration sensors are popular with researchers due to the ease of installation and lower cost [18]. In the respect of signal processing techniques for detecting chatter, usually, the simplest method is to determine a magnitude threshold value in the time domain or the frequency domain. Yeh and Lai [3] suggested the standard deviation value of cutting force as the reference chatter threshold. In addition, wavelet analysis, expert systems, fuzzy logic, and artificial neural networks are also adopted [18]. Nicolescu [19] introduced a stochastic model to estimate the dynamic interaction between the cutting process and the workpiece with the data of cutting force and acceleration. Cardi et al. [2] proposed the phase difference between the cutting force and the workpiece velocity to classify the transition from stable cutting to chatter, and used a data-driven technique to predict the workpiece displacement during chatter. Three ratios of the measured cutting forces were introduced to classify the cutting states in [20]. With this method the states of cutting were well identified regardless of the cutting conditions. However, those detection algorithms rely on empirically selected thresholds that cannot be valid over a wide range of cutting conditions.

A substantial amount of effort has been made on chatter in machining processes, however, the dynamic behavior while turning the challenging slender workpieces has seldom been studied systematically. To the authors' knowledge, much prior research focused on the turning dynamics of flexible workpieces at some discrete and specific cutting locations using the simplified orthogonal cutting models. In practice, however, the tool keeps engaged with the workpiece at the point of cut and moves along the longitudinal axis of the workpiece continuously during an entire cutting pass. Moreover, the experimental observations that when chatter occurs at some cutting position during turning operations of thin walled workpieces it will last for a period of time has been described in [21, 22]. The analogous phenomenon also happened in our previous slender workpieces turning experiments [23]. A lack of investigation into the nature of the transition from stable cutting to chatter in turning of a flexible workpiece still exists. Thus, the chatter stability and characteristics in straight turning of a slender long workpiece should be investigated from the global perspective rather than from the local perspective, which in turn creates a time-variant cutting system.

The primary objective of the present paper is to formulate a dynamic model of a clamped-simply supported slender workpiece in straight turning. Modeling the onset of chatter enables to predict chatter emergence or detect it as soon as it happens so as to increase the time available for the response of the control system. An analytical model for chatter onset prediction is introduced. The dynamic characteristics of the cutting system in machining are analyzed theoretically and experimentally. First an SDOF regenerative chatter model of a flexible rod is constructed. Then the chatter stability curve for an entire cutting pass is deduced and the chatter behavior during cutting is predicted. Finally, a series of experimental trials were performed extensively, and the comparison of the experimental and theoretical results is discussed.

## 2. Formulation of chatter prediction model

This paper focuses on the case of a uniform slender shaft with length  $L$  and diameter  $D$ , which is clamped by the chuck at one end and simply supported by a live center at the other end. Considering lathes are almost exclusively designed to have sufficient stiffness nowadays, thus it is reasonable to assume that the frame of the machine tool and the tool are rigid with respect to the slender workpiece. The rod is rotating at spindle speed  $\Omega$  and the cutting tool moves along the Z-axis with feedrate  $f$ .

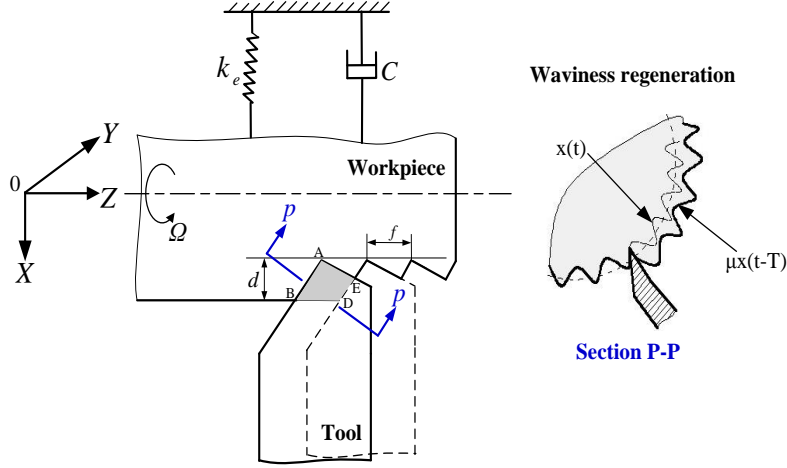


Fig. 1. SDOF chatter model of straight turning of a long slender rod.

### 2.1 SDOF chatter model and its vibration features

Regenerative chatter refers to the cutting force variation due to the dynamic chip thickness formed by regeneration of waviness on both sides of the chip surface. The chatter vibration of workpiece in the X-axis direction is analyzed because the fluctuations in area of the cut induced by the radial vibration of the workpiece contribute mainly to the occurrence of chatter vibrations. Regard the flexible workpiece as an SDOF system as illustrated in Fig. 1, the corresponding mathematical chatter model is a delayed differential equation (DDE),

$$\ddot{x} + 2\omega_n \zeta \dot{x} + \omega_n^2 x = \frac{K_f \omega_n^2 d}{k_e} [\mu x(t-T) - x(t)] \quad (1)$$

where the equivalent modal parameters  $k_e$ ,  $\zeta$ ,  $\omega_n$  can be achieved via modal analysis along with numerical analysis,  $C$  is the damping coefficient,  $K_f$  is a constant coefficient related to cutting conditions,  $d$  is the depth of cut,  $\mu = DE/AB$  is the overlap factor, and  $T = 60/\Omega$  is the time delay.

Solving the DDE by the use of the Laplace transform, one can obtain the corresponding stability chart expressions as follows,

$$\left. \begin{aligned} \Omega(\omega) &= \frac{60\omega}{2j\pi + \theta} \quad j = 0, 1, 2, \dots \\ d_{\text{lim}}(\omega) &= -\frac{2\zeta\omega k_e}{K_f \mu \omega_n \sin \theta} \end{aligned} \right\} \quad (2)$$

where  $\theta = \sin^{-1} \frac{2\zeta\omega_n\omega}{\mu\sqrt{(2\zeta\omega_n\omega)^2 + (\omega_n^2 - \omega^2)^2}} - \cos^{-1} \frac{\omega_n^2 - \omega^2}{\sqrt{(2\zeta\omega_n\omega)^2 + (\omega_n^2 - \omega^2)^2}}$ , and  $\omega$  is the chatter frequency.

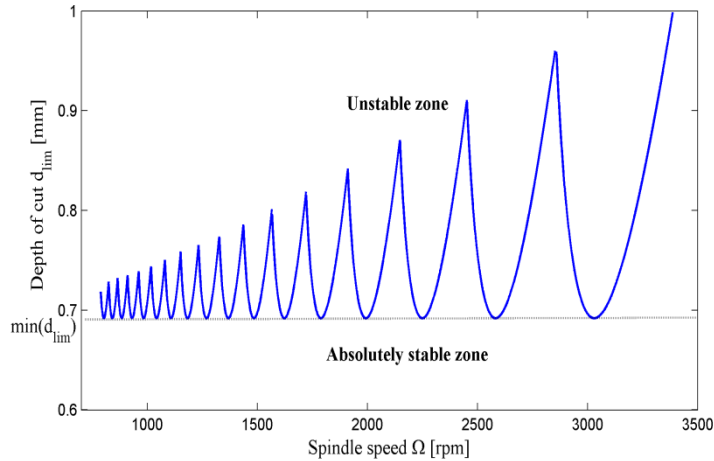


Fig. 2. Stability lobes of the SDOF chatter system.

To gain an indepth knowledge of the relationships in Eq. (2), a typical stability lobe for a cutting system can be illustrated in Fig. 2, where the modal parameters are from the following experimental test:  $\omega_n = 272$  Hz,  $\zeta = 0.072$ ,  $k_e = 4.2 \times 10^6$  N/m. If cutting parameters locate below the boundary curves, the cutting operation is stable; above them, chatter vibrations may arise in turning processes.

When unstable chatter appears, the amplitude of vibration responses enlarges significantly but confined by the loss of contact [24] in the practical cutting processes. Variance analysis is effective for mapping the trend line of the change in vibration amplitude. In the frequency domain, the critical chatter frequency presents and is generally higher than the natural frequency of the workpiece  $\omega_n$ . Moreover, the frequency value of the dominant vibration is distinctively higher. These inherent changes in vibrations, therefore, can be based on for developing an online detection method of the occurrence of the unstable vibrations.

From Fig. 2, it is seen that the lobe structure is relevant to the specific machining parameters, and the minimum critical  $doc$ ,  $\min(d_{lim})$ , is identical for each lobe. Thus, only  $\min(d_{lim})$  is considered to estimate the stable domain. The value of  $\min(d_{lim})$  can be found for some critical cutting speeds. Thus, the asymptotic borderline of stability can be drawn by connecting each lowest point of the lobes as seen in Fig. 2. Below this horizontal line the machining system is absolutely stable.

The overlap factor  $\mu$  is close to be unity for lower feedrate is widely applied in turning process [25]. Then the minimum critical  $doc$   $\min(d_{lim})$  can be further deduced by claculating the derivative of  $d_{lim}$  with respect to  $\omega$  in Eq. (2), which has

$$\min(d_{lim}) = \frac{2\zeta(1+\zeta)k_e}{K_f} \quad (3)$$

In essence, this analytical expression is consistent with the results in [26,27]. It is clear that  $\min(d_{lim})$  is independent of the chatter frequency, and is directly proportional to the stiffness  $k_e$  of the SDOF chatter system.

## 2.2 Location-dependent stiffness of the cutting system

Obviously, the stiffness of the workpiece at the cutting point is varying with the tool moving along the Z-axis during a turning operation. It has been proven that an Euler-Bernoulli beam model is adequate for conventional machining of slender workpieces, and that the dynamic effects due to rotation and shear deformation are simply significant for ultra-high spindle speeds or the length-to-diameter ratio of the workpiece is less than about 10 [28, 29]. Therefore, the Euler-Bernoulli beam model is adopted to analyze the dynamics of the slender shaft here.

The governing equation of motion has the form<sup>[30]</sup>

$$EI \frac{\partial^4 x(z,t)}{\partial z^4} + \rho A \frac{\partial^2 x(z,t)}{\partial t^2} = F\delta(z,t) \quad (4)$$

where  $x(z,t)$  is the transverse displacement,  $F\delta(z,t)$  is the moving cutting force,  $\rho A$  is the mass per unit length, and  $EI$  is the flexural rigidity.

First, the following non-dimensional variables are introduced for simplicity

$$k^* = \frac{z}{L}, s^* = \frac{L}{D}, \tau^* = \left(\frac{EI}{\rho AL^4}\right)^{1/2} t, \mu^* = \frac{f}{(v_1)_{cr}}. \quad (5)$$

where  $(v_1)_{cr} = \left(\frac{EI}{\rho AL^2}\right)^{1/2} \alpha_1$  is defined as the first critical feedrate, and  $\alpha_1 = 3.927$  is associated with the fundamental frequency of the workpiece:

$$\omega_n = \alpha_1^2 \sqrt{\frac{EI}{\rho AL^4}} \quad (6)$$

Then, by using the separation of variables, the partial differential equations (4) can be solved to yield an analytical response to the traveling cutting force:

$$\begin{aligned}
x(z,t) = \sum_{j=1}^{\infty} W_j(z) T_j(t) = \frac{64F}{E\pi L} \sum_{j=1}^{\infty} \frac{B_j^2 s^{*4}}{\alpha_j^2} \{ & [\sin(\alpha_j k^*) - \sinh(\alpha_j k^*)] - R_j [\cos(\alpha_j k^*) - \cosh(\alpha_j k^*)] \} \\
& \times \left\{ \frac{1}{\alpha_j^2 - \mu^{*2} \alpha_1^2} [\sin(\mu^* \tau^* \alpha_j \alpha_1) - R_j \cos(\mu^* \tau^* \alpha_j \alpha_1)] - \frac{1}{\alpha_j^2 + \mu^{*2} \alpha_1^2} [\sinh(\mu^* \tau^* \alpha_j \alpha_1) - \right. \\
& \left. R_j \cosh(\mu^* \tau^* \alpha_j \alpha_1)] + \frac{2\mu^{*2} \alpha_1^2}{\alpha_j^4 - \mu^{*4} \alpha_1^4} \left[ -\frac{\mu^* \alpha_1}{\alpha_j} \sin(\tau^* \alpha_j^2) + R_j \cos(\tau^* \alpha_j^2) \right] \right\}
\end{aligned} \tag{7}$$

where  $\alpha_j \approx (j+1/4)\pi$ ,  $B_j \approx 1.0$ ,

and  $R_j = (\sin \alpha_j - \sinh \alpha_j) / (\cos \alpha_j - \cosh \alpha_j)$ .

According to Eq.(7), it can be proved that the first mode shape is generally dominant in the modal participation of the mode shapes. And since feedrate used in conventional turning operations is quite small in comparison with  $(v_1)_{cr}$ , the dynamic response of the shaft under the traveling cutting force is analogous with the static deflection under concentrated force acting at different locations.

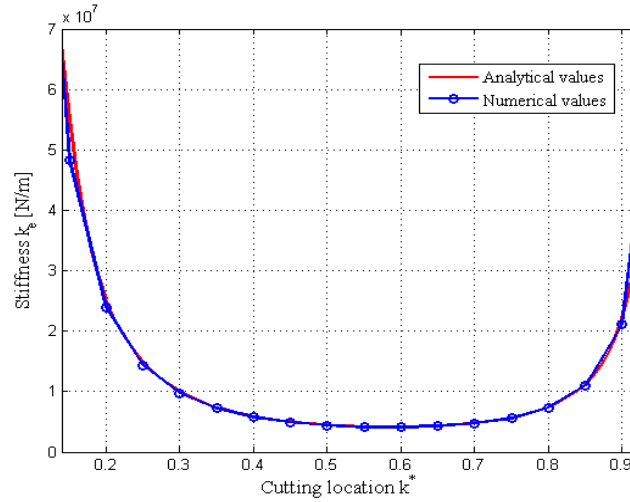


Fig. 3. Static flexural stiffness of the machined rod at different cutting positions.

Lastly, through dividing both sides of Eq. (7) by the cutting force  $F$ , the static flexural stiffness ( $F/x$ ) of the slender shaft at different axial positions can be derived. To prove the analytical results true, the numerical stiffness values were calculated by the finite element method as well. The values from the two different methods are close, as given in Fig.3. The following parameters were used for calculation:  $E = 206000$  MPa,  $L = 460$  mm,  $D = 25$  mm,  $\rho = 7860$  Kg/m<sup>3</sup>. Also, the analytical stiffness curve resembles the ones attained experimentally in [31, 32]. Comparatively, it is seen that the location of the workpiece near the chuck holds much higher stiffness since the boundary condition at the chucking jaw position was assumed as a fixed end.

### 3. Chatter onset prediction and detection

According to the above analysis, the stiffness along the workpiece is location-dependent and the first vibration mode is only considered, thus the modal parameters in Eq. (1) are varying during turning process. The stiffness variation along the workpiece can be achieved by using Eq. (7), the equivalent mass of the rod reduced to any point along the length can be calculated from the stiffness values and the natural frequency by Eq. (6).

Since  $doc$  is the decisive machining parameter for the generation of chatter in turning operations, a different critical  $doc$   $d_{lim}$  corresponding to a varying value of stiffness, can be obtained through Eq. (3). As a result, a stability chart for an entire cutting pass can be plotted with respect to the value of the critical  $doc$  and the axial coordinate of the cutting location, as shown in Fig. 4.

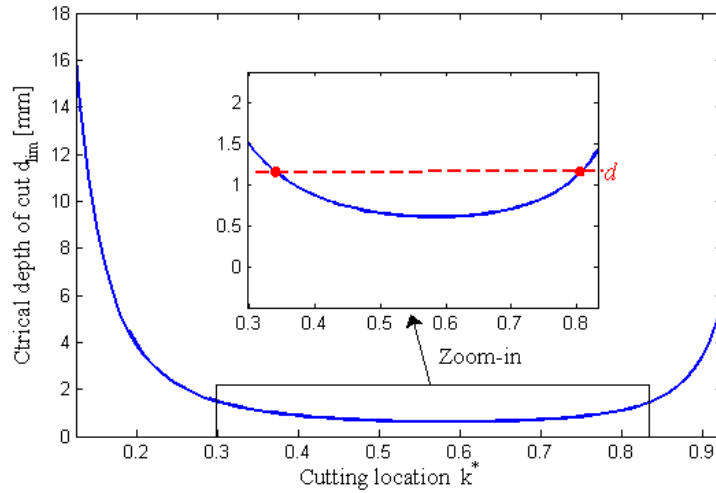


Fig. 4. Chatter stability chart for an entire individual cutting pass.

Mathematically, the entire stability graph is a convex function. If the set  $doc$   $d$  is greater than the minimum value of  $d_{lim}$ , there will be two intersection points of the horizontal line and the stability curve, as shown in Fig. 4. It indicates that when the cutting tool, no matter which direction the turret chatter vibrations may occur, and if no any control measures are taken the unstable state will last for a period of time until another cutting location whose  $d_{lim}$  is also equal to  $d$  is reached. After that, the cutting returns to stable level again. In theory, if  $d$  is less than the minimum value of  $d_{lim}$  which approximately occurs at the location  $k^* = 0.58$ , the cutting will constantly be stable and chatter will not happen during a cutting pass.

Once chatter evolves, it is necessary to confirm its features and detect it quickly. Combining the vibration response of the SDOF model with the variant stiffness along the workpiece, it can be predicted that the chatter frequency will vary during the cutting process with traveling cutting excitations. Besides chatter frequency, the frequency of the free vibration response caused by the initial contact of the tool and workpiece will decay soon due to damping effect. But the frequencies, representing the phenomena of the unbalanced rod or spindle rotation and the friction between the cutting tool edge and the machined chip surface, could permanently exist for an entire cutting pass. Accordingly, an adaptive threshold determined through instant comparison of the features of the acquired signal with the stored stable cutting signal may be more effective and efficient for chatter detection. Initially, the variance and the dominant frequency information of the stable cutting signals were calculated and saved in a reference library. Thereafter, the following newly acquired data were compared with this reference. Alarm was triggered off when both the variance and spectrum satisfy the criteria quantitatively. The proposed method for chatter detection is shown in Fig. 5.

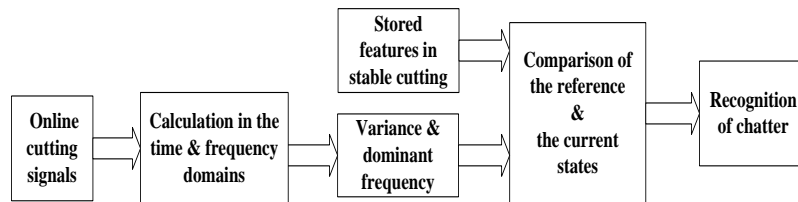


Fig. 5 Block diagram of chatter detection.

## 4. Experiments and discussion

This section deals with the validation of the prior theoretical analysis results. The experimental setup is shown in Fig. 6. Experimental trials were carried out on a CKA6150 conventional lathe. The workpiece with the length 460mm and diameter 25mm was clamped by a three jaw chuck at one end and simply supported by a live center at the other end. The material of the workpiece was 1045 steel. The carbide insert tool was used. Its nose angle, nose radius, and clearance angle were  $55^\circ$ ,  $0.4\text{mm}$ , and  $7^\circ$ ,

respectively. Two accelerometers and two proximity transducers were employed to continuously acquire the machining states. The accelerometers were adhered to the tailstock and turret, respectively. One proximity sensor was fixed to measure displacement of the workpiece in X direction. The other one was perpendicular to it. The portable data acquisition system, CoCo-80, picked up vibrations with the sample rate of 1600 Hz. In addition to the use of cutting fluid, for each experimental rod a fresh cutting tool was utilized to eliminate the tool wear effect on the dynamic behavior of the workpiece. Table 1 gives the designed conditions for the tests.

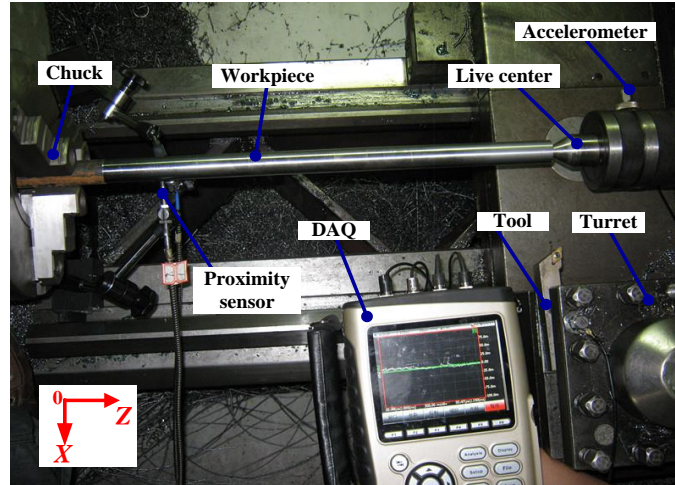


Fig. 6. Experimental setup.

For the analytical chatter stability calculation, the cutting coefficient and the damping ratio were estimated to be  $K_f = 937\text{MPa}$  on the basis of the experimental results obtained in [8] and  $\zeta = 0.072$  from Fig. 7, respectively. The actual locations of chatter onset were identified by combining the features of the continuous vibration records with the chatter marks left on the surface of the workpieces. The vibration features were extracted in accordance with the variance and spectrum of the acquired signals. Two different feed directions, along +Z and -Z axes, were considered. Also, for each direction two different spindle speeds were conducted to compare their effect on the chatter prediction results. For both cases the location is expressed in term of the ratio of the distance from the chuck to the total length of the workpiece. The experimental locations of chatter onset are compared with the analytical prediction in Fig. 8.

Table 1. Programmed conditions for chatter onset tests.

| Case | Depth of cut $d$ (mm) | Spindle speed $\Omega$ (rpm) | Feedrate $f$ (mm/rev) | Feed direction | Diameter $D$ and length $L$ (mm) |
|------|-----------------------|------------------------------|-----------------------|----------------|----------------------------------|
| 1    | 0.6/0.8/.../1.8       | 1200/450                     | 0.1                   | +Z             | 25/460                           |
| 2    | 0.6/0.8/.../2         | 1200/450                     | 0.1                   | -Z             | 25/460                           |



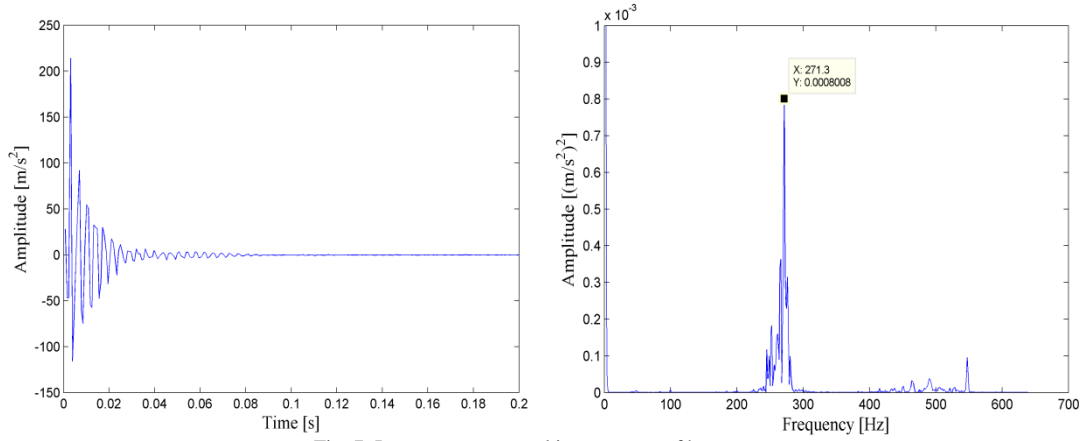


Fig. 7. Impact response and its spectrum of hammer test.

As expected in theory, the increase of the *doc* could make the chatter onset along the workpiece close to the chuck or tailstock, as seen in Fig. 8. With the same depths of cut employed, the distance from the chatter onset location to the chuck end in the case of feeding along +Z direction is further than that from the location to the tailstock end in the case of feeding along -Z direction. This attributes mainly to the asymmetric boundary conditions at the two ends of the workpiece. In the meantime, it was interesting to note that the strategy that the cutting tool moves along +Z axis was beneficial to cutting stability.

With respect to the influence of the spindle speeds, it has been observed that the lower spindle speed caused the chatter onset location further away from the two ends of the rod in comparison with the higher speed, and the chatter vibrations during the lower speed cutting were not strong as the higher speed. These phenomena manifest that reducing the cutting speed is more advantageous to avoid chatter occurrence in turning of slender long workpieces. At  $\Omega=1200\text{rpm}$ , the critical *doc*,  $d_{lim}$ , with respect to cutting locations was also calculated by Eq. (2). Apparently, the entire stability curve based on  $d_{lim}$  is constantly above the analytical curve through  $\min(d_{lim})$ , as shown in Fig. 8. The percentage error, the ratio of the difference between the analytical and actual chatter onset locations to the analytical chatter onset location, was calculated. For the case of  $\Omega=1200\text{rpm}$  the average percentage error is 8.95%, yet the error increases to 13.14% for the case of  $\Omega=450\text{rpm}$ . This can be considered as the result of the process damping effect which has a significant influence on the improvement of the machining stability at lower spindle speeds [18]. Besides, the fact that the practical clamping conditions are different from the theoretical boundary conditions considered during the analytical calculation, could contribute to the predictive error as well.

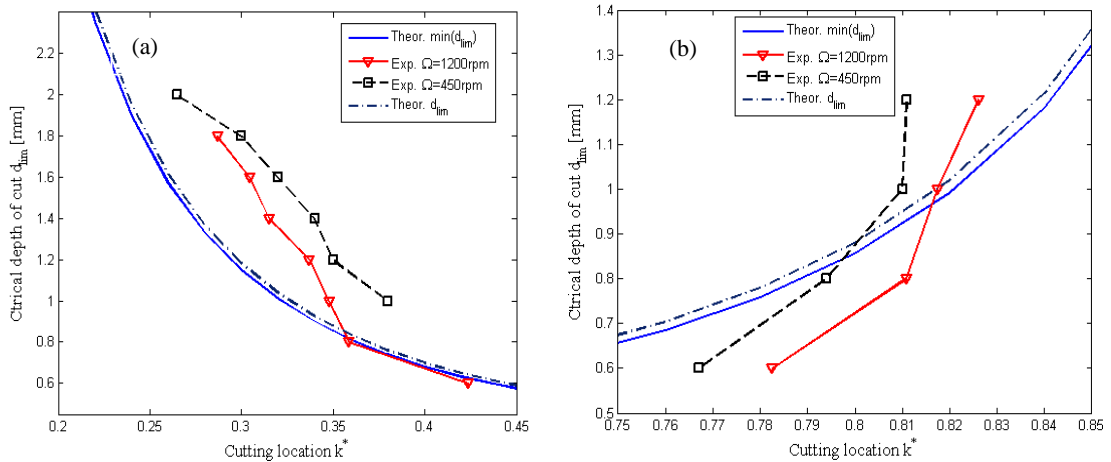


Fig. 8. Comparison of the experimental chatter onset locations and the theoretical results: (a) tool feeds along +Z direction; (b) tool feeds along -Z direction

Figure 9 illustrates a typical machined surface of a workpiece after an entire cutting pass and the corresponding acceleration measurements. The machining parameters used are as follows:  $d=1\text{mm}$ ,  $\Omega$

=1200rpm,  $f=0.1$ mm/rev from the tailstock to the chuck end. From Figs. 9(a) and 9(b), it has been found that the cutting condition was generally stable at the beginning of the turning process; when the cutting tool arrived at some specified location, chatter occurred and the amplitude of vibration enlarged, and then continued in the following period of time until another specified location was reached; finally chatter disappeared and the stable cutting was restored. This experimental observation is in good agreement with the theoretical inference in the prior section.

The comparative results of the variance and spectrum of the acquired acceleration are given in Figs. 9(c) and 10. In the time domain, the onset of chatter seems to be a gradual process; while in the frequency domain the dominant frequency shows a jump, as seen in Fig. 9(c). This demonstrates that spectrum is more sensitive to detection of chatter vibration than variance. When the cutting is stable, the spindle rotation frequency ( $f_{SR}=20.3$ Hz) and its higher harmonics corresponding to the inevitable unbalance of the rod or spindle with deviation of center of mass arise; when chatter happens, the dominant frequency shifts to the critical chatter frequency ( $f_c=282.8$ Hz) which is a little above the natural frequency of the workpiece ( $\omega_n=272$ Hz) obtained by the hammer test after the cutting pass (see Fig. 7). The sidebands around  $f_c$  are spaced at 20.3Hz due to amplitude modulation, as shown in Fig. 10. The similar results can be obtained by computing the spectrum of the displacement signal.

In chatter detection respect, the accelerometers were utilized in the experiments. The proposed chatter detection module mainly consists of frequency extraction, new frequency search, variance calculation, and variance comparison functions. Take the case in Fig. 9(b) as an example, at the beginning of cutting the first  $M_1$  (default 3) principal frequency components and the variance value of the vibration signals were extracted and saved as the reference. Thereafter, the following frames of newly acquired data were calculated and compared with this reference. At  $t=37.6$ s as seen the dashed box in Fig. 9(b), new frequencies  $f_c$  and its sidebands occurred. Also, the variance of the data was more than  $M_2$  (default 2.5) times greater than the referred value. Chatter alarm was on until  $t=158.2$ s. To overcome the misjudgement resulted from the mixed impulse signals due to the hard impure particle in workpiece or strong noises on the shop floor, the delay strategy that the impulse occurring for consecutive  $M_3$  (default 3) times will be regarded as a chatter candidate, is employed. Additionally, overlap processing was applied to improve the computing efficiency. The overlap ratio  $M_4$  (default 25%) was set to be 50% in the cutting experiments. When the cutting conditions change, the reference database needs to be refreshed. Under various cutting conditions the chatter threshold algorithm has shown high reliability.

From Fig. 9(c), it is shown that the chatter frequency varies slightly during the chatter-lasting period. This is consistent with the analytical conclusion of the proposed model. And the variation pattern is similar to the variation of the natural frequency of the workpiece during machining in [11]. This characteristic as well as the heterogeneity of the chatter marks left on the work surface demonstrates the parameters of the cutting system underwent time variation during turning of the flexible rod.

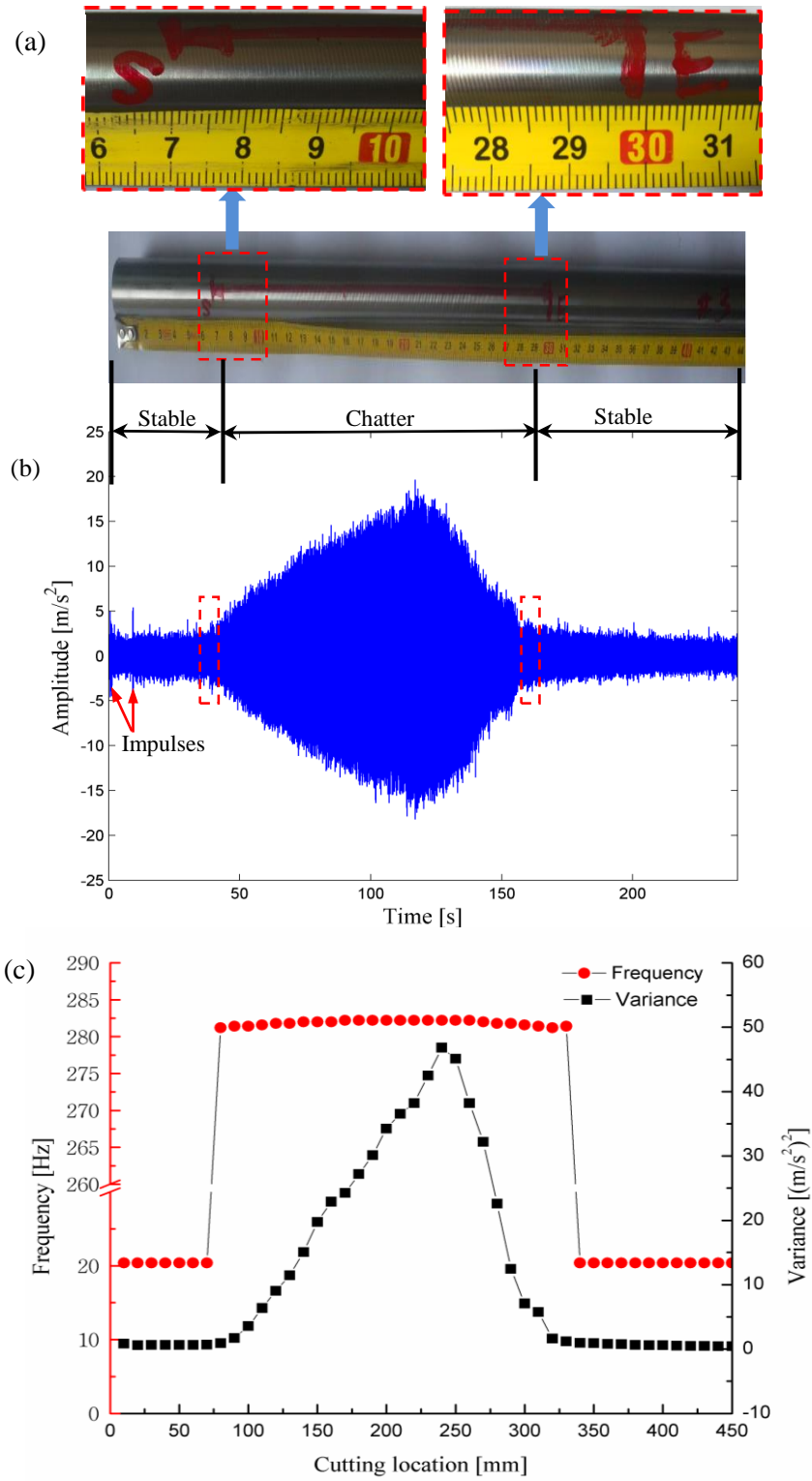


Fig. 9. Workpiece surface quality and acceleration signals analysis: (a) chatter-lasting manifestation of the work surface; (b) chatter-lasting manifestation of the acceleration; (c) spectrum and variance analysis.

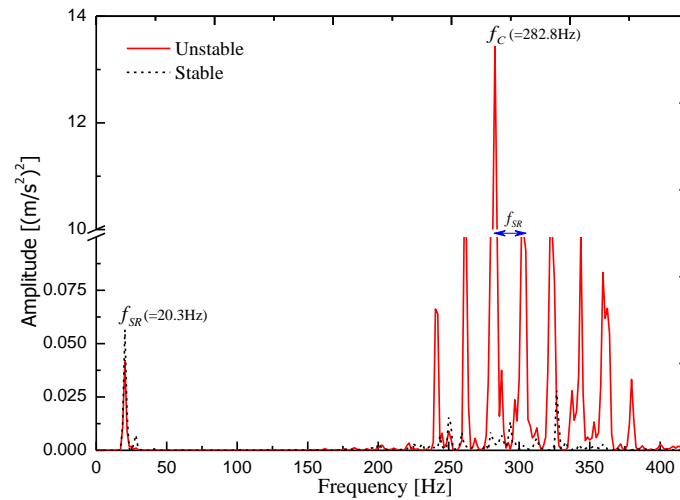


Fig. 10. Spectral comparison of acceleration signals in stable and unstable cutting states.

## 5. Conclusions

In this study, a predictive chatter model of tailstock supported slender workpieces in straight turning which includes the effect of the traveling tool position along the longitudinal direction of the workpiece during machining, has been developed. By using stability analysis of the proposed model, the critical cutting condition and the chatter onset location can be determined. Also, the inference of chatter lasting effect that when chatter occurs at some cutting location it will continue for a period of time until another specified location was reached, can be drawn. A series of experimental trials were extensively performed to verify the chatter model. The experimental observation was in good agreement with the theoretical inference. The effect of *doc*, feed direction and spindle speed on the chatter onset was also discussed. The difference between the predicted tool locations and the experimental results was within 9% at high speed cutting.

In addition, the spectrum and variance of the acceleration signals were calculated to summarize the chatter vibration features in turning a flexible rod. It is shown that the corresponding dominant vibration frequency shifts from the spindle rotation frequency or its harmonics to the critical chatter frequency that slightly varies during the chatter-lasting period, when the cutting operation transfers from stable to chattering state. Accordingly, a relative threshold for chatter detection is suggested to improve the self-adaptiveness of the chatter monitoring technique for various turning conditions.

## Acknowledgments

This work has been partially supported by the Qualified Personnel Foundation of TYUT (1205-04020203), by Shanxi Key Science and Technology Project (MJ2014-06), and by the Open Research Fund of the MCME lab (2015-01).

## References

- [1] Y. Altintas, M. Weck, Chatter stability of metal cutting and grinding, *CIRP Annals - Manufacturing Technology* 53(2) (2004) 619-642.
- [2] A.A. Cardi, H.A. Firpi, M.T. Bement, S.Y. Liang, Workpiece dynamic analysis and prediction during chatter of turning process, *Mechanical Systems and Signal Processing* 22 (2008) 1481-1494.
- [3] L.J. Yeh, G.J. Lai, A study of the monitoring and suppression system for turning slender workpieces, *Proceedings of the Institution of Mechanical Engineers, Part B: Journal of Engineering Manufacture* 209(3) (1995) 227-236.
- [4] L. Tian, J. Wu, Z. Xiong, H. Ding, Active chatter suppression in turning of low-rigidity workpiece by system matching, in: *Proceedings of Intelligent Robotics and Applications- 8<sup>th</sup> International Conference, ICITA 2015*, 2015, pp. 609-618.
- [5] S.A. Tobias, *Machine Tool Vibration*, Blackie and Sons Ltd., London, 1965.
- [6] E. Marui, S. Ema, S. Kato, Chatter vibration of lathe tools Part 1: General characteristics of chatter

- vibration, *ASME Journal of Engineering for Industry* 105 (1983) 447-454.
- [7] R.Y. Chiou, S.Y. Liang, Chatter stability of a slender cutting tool in turning with tool wear effect, *International Journal of Machine Tools and Manufacture* 38(4) (1998) 315-327.
- [8] G. Urbikain, L.N. Lopez de Lacalle, F.J. Campa, A. Fernandez, A. Elias, Stability prediction in straight turning of a flexible workpiece by collocation method, *International Journal of Machine Tools and Manufacture* 54-55 (2012) 73-81.
- [9] W.F. Lu, B.E. Klamechi, Prediction of chatter onset in turning with a modified chatter model, in: *Proceedings of ASME WAM PED-Vol. 44*, 1990, pp.237-251.
- [10] Z.C. Wang, W.L. Cleghorn, Stability analysis of spinning stepped-shaft workpieces in a turning process, *Journal of Sound and Vibration* 250(2) (2002) 356-367.
- [11] S.D. Yu, V. Shah, Theoretical and experimental studies of chatter in turning for uniform and stepped workpieces, *Journal of Vibration and Acoustics* 130(6) (2008) 1005-1018.
- [12] C.K. Chen, Y.M. Tsao, A stability analysis of turning a tailstock supported flexible work-piece, *International Journal of Machine Tools and Manufacture* 46(1) (2006) 18-25.
- [13] C.K. Chen, Y.M. Tsao, A stability analysis of regenerative chatter in turning process without using tailstock, *The International Journal of Advanced Manufacturing Technology* 29(7-8) (2006) 648-654.
- [14] L. Vela-Martinez, J.C. Jauregui-Correa, E. Rubio-Cerda, H.R. Gilberto, L.G. Alejandro, Analysis of compliance between the cutting tool and the workpiece on the stability of a turning process, *International Journal of Machine Tools and Manufacture* 48(9) (2008) 1054-1062
- [15] M. Sekar, J. Srinivas, K. Kotaiah, S. Yang, Stability analysis of turning process with tailstock-supported workpiece, *The International Journal of Advanced Manufacturing Technology* 43 (2009) 862-871.
- [16] S. Li, Z.Q. Li, M. Zhang, Chatter stability modeling and simulation for long slender shaft turning operation, *Applied Mechanics and Materials* 155-156 (2012) 1227-1231.
- [17] A. Otto, F.A. Khasawneh, G. Radons, Position-dependent stability analysis of turning with tool and workpiece compliance, *The International Journal of Advanced Manufacturing Technology* 79 (2015) 1453-1463.
- [18] M. Siddhpura, R. Paurobally, A review of chatter vibration research in turning, *International Journal of Machine Tools and Manufacture* 61 (2012) 27-47.
- [19] C.M. Nicolescu, On-line identification and control of dynamic characteristics of slender workpieces in turning, *Journal of Materials Processing Technology* 58 (4) (1996) 374-378.
- [20] S. Tangjitsitharoen, In-process monitoring and detection of chip formation and chatter for CNC turning, *Journal of Materials Processing Technology* 209(10) (2009) 4682-4688.
- [21] J.Y. Chang, G.J. Lai, M.F. Chen, A study on the chatter characteristics of the thin wall cylindrical workpiece, *International Journal of Machine Tools and Manufacture* 34(4) (1994) 489-498.
- [22] K. Mehdi, J.F. Rigal, D. Play, Dynamic behavior of a thin-walled cylindrical workpiece during the turning process, Part 2: Experimental approach and validation, *ASME Journal of Manufacturing and Engineering* 124 (2002) 569-580.
- [23] K. Lu, M. Jing, Y.Q. Zhang, H. Liu, Industrial applications of a system for chatter stability prediction and monitoring, in: *Proceedings of ASME 2011 International Mechanical Engineering Congress and Exposition*, 2011, pp. 839-845.
- [24] H.M. Shi, S.A. Tobias, Theory of finite amplitude machine tool instability, *International Journal of Machine Tool Design and Research* 24 (1) (1984) 45-69.
- [25] G. Stepan, Modelling nonlinear regenerative effects in metal cutting, *Philosophical Transactions of the Royal Society of London: Mathematical, Physical, and Engineering Sciences* 359(1781) (2001) 739-757.
- [26] E. Budak, L.T. Tunc, A new method for identification and modeling of process damping in machining, *ASME Journal of Manufacturing and Engineering* 131 (2009) 1-10.
- [27] M. Zatarain, I. Bediaga, J. Munoa, T. Insperger, Analysis of directional factors in milling: importance of multi-frequency calculation and of the inclusion of the effect of the helix angle, *The International Journal of Advanced Manufacturing Technology* 47 (2010) 535-542.

- [28] C.W. Lee, R. Katz, A.G. Ulsoy, R.A. Scott, Modal analysis of a distributed parameter rotating shaft, *Journal of Sound and Vibration* 122(1) (1988) 119-130.
- [29] R. Katz, C.W. Lee, A.G. Ulsoy, R.A. Scott, The dynamic response of a rotating shaft subject to a moving load, *Journal of Sound and Vibration* 122(1) (1988) 131-148.
- [30] K.B. Lu, M. Jing, H. Liu, C. Cong, Dynamic analysis of slender shaft in twin-spindle turning, *Applied Mechanics and Materials* 48-49 (2011) 448-454.
- [31] E.I. Rivin, H. Kang, Improvement of machining conditions for slender parts by tuned dynamic stiffness of tool, *International Journal of Machine Tools and Manufacture* 29(3) (1989) 361-376.
- [32] S.T. Chiriacescu, *Stability in the Dynamics of Metal Cutting*, Elsevier Science Publishers, 1990.